JOURNAL OF VIROLOGY, Sept. 1994, p. 5781–5791
0022-538X/94/$04.00+0

Vol. 68, No. 9

Genetic Analysis of the nsP3 Region of Sindbis Virus: Evidence for Roles in Minus-Strand and Subgenomic RNA Synthesis

MARK W. LaSTARZA, JULIE A. LEMM, AND CHARLES M. RICE*

Department of Molecular Microbiology, Washington University School of Medicine, St. Louis, Missouri 63110-1093

Received 16 March 1994/Accepted 31 May 1994

Sindbis virus nonstructural polyproteins and their cleavage products are believed to be essential components of viral RNA replication and transcription complexes. Although numerous studies have investigated the effect of mutations in nsP1-, nsP2-, and nsP4-coding regions on Sindbis virus-specific RNA synthesis, relatively little is known about the function of the region encoding nsP3. nsP3 is a phosphoprotein comprising two regions: an N-terminal portion which is highly conserved among alphaviruses and a C-terminal portion which is not conserved, varying both in sequence and in length. We have constructed a library of random linker insertion mutations in the nsP3-coding region and characterized selected viable mutants. Initially, 126 mutants containing insertions in the conserved region and 23 with insertions in the nonconserved region were screened for temperature-sensitive (*ts*) plaque formation or for significant differences in plaque morphology. All nonconserved-region mutants were similar to the parental virus, whereas 13 of those in the conserved region were either *ts* or exhibited altered plaque phenotypes. Ten of these 13 mutants were *ts* for plaque formation as well as RNA accumulation at 40°C. Highly *ts* mutants CR3.36 and CR3.39 were defective in their ability to synthesize minus-strand RNAs at the nonpermissive temperature. The CR3.36 and CR3.39 insertion mutations localized to different regions near nsP3 residues 58 and 226, respectively. CR3.39 was able to complement *ts* mutants from Sindbis virus complementation groups A, B, F, and G. Another mutant isolated from the library, CR3.34, while not *ts* for plaque formation or RNA synthesis, formed smaller plaques and was defective in subgenomic RNA synthesis at all temperatures examined. These results suggest a role for nsP3 or nsP3-containing polyproteins in the synthesis of viral minus-strand and subgenomic RNAs.

Sindbis virus (SIN) is an enveloped plus-strand RNA virus in the genus *Alphavirus* and family *Togaviridae* (see reference 49 for a review). Upon infection, the genomic RNA serves as both the mRNA for synthesis of the viral nonstructural proteins and the template for synthesis of complementary minus-strand RNA. Newly synthesized minus-strand RNA in turn functions as the template for both synthesis of plus-strand genomic RNAs and transcription of subgenomic RNAs, which are translated to produce the viral structural proteins. Synthesis of these viral RNAs during the viral replication cycle in vertebrate host cells is highly regulated. The rate of viral plus-strand RNA synthesis increases during the early stages of infection, reaches a maximal level, and then continues at this rate until late in infection (46, 47) when host cells begin to deteriorate (8). In contrast, minus-strand RNA synthesis reaches a maximal rate early in infection and then rapidly decreases to barely detectable levels (46). The timing of minus-strand shutoff coincides with maximal plus-strand synthesis, suggesting that the concentration of minus-strand templates may limit plus-strand synthesis. However, studies of mutants defective in minus-strand shutoff suggest that other factors besides minus strands can limit plus-strand synthesis rates (43). The ratio of genomic to subgenomic RNA synthesis is also regulated and increases during the course of infection (52). Although models have been proposed (5), the mechanisms which regulate these template-specific initiation events are not well understood.

SIN nonstructural polyproteins and their cleavage products, translated from genome-length plus-strand RNAs, are essential components of viral RNA replication and transcription complexes. The SIN nonstructural proteins are initially synthesized as two polyproteins, designated P123 and P1234 (16). P1234 is synthesized in smaller quantities than P123 since its synthesis is dependent on readthrough of an in-frame opal termination codon following the nonstructural protein nsP3 (33, 56). The papainlike proteinase domain responsible for cleavage of these polyproteins resides in the C-terminal domain of the nsP2 protein (6, 17), and the processing pathways are complex and regulated by the cleavage site specificities and *cis-trans* properties of the various nsP2-containing proteinases (5, 17, 50; for a review, see reference 59). Early in infection, cleavage of P1234 at the 3/4 bond is believed to occur in *cis*. Cleavage at the 1/2 and 2/3 sites appears to occur in *trans* such that efficient processing at these sites depends on the concentration of *trans*-acting proteinases. Later in infection, mainly processed products nsP1, nsP2, and nsP3 are observed, although polyprotein P34 accumulates as a consequence of inactivation of proteinases which can cleave at the 3/4 site.

Possible roles for different portions of the nsP-coding region in RNA replication have been postulated on the basis of limited sequence homology with known host and viral enzymes (1, 19), biochemical assays, and numerous studies using SIN mutants. Recent results also suggest that distinct functions may be performed by uncleaved polyproteins as opposed to processed nonstructural proteins (27–29, 51, 62). The nsP1 region encodes a methyltransferase activity (35, 36) and possible capping functions (48), and mutations in this region can result in a temperature-sensitive (*ts*) defect in minus-strand synthesis, probably at the level of initiation (14, 46, 61). The N-terminal portion of the nsP2-coding region contains nucleoside triphosphate binding and helicase motifs (9), and, as mentioned above, the C-terminal portion is a papainlike proteinase domain involved in nonstructural region processing (53). Mutations in the nsP2 region can result in aberrant processing (15),

* Corresponding author. Mailing address: Department of Molecular Microbiology, Washington University School of Medicine, Box 8230, 660 S. Euclid Ave., St. Louis, MO 63110-1093. Fax: (314) 362-1232. Electronic mail address: rice@borcim.wustl.edu.

defects in subgenomic RNA synthesis (14, 44), and *ts* resumption of minus-strand synthesis (45). The nsP4 region contains motifs characteristic of RNA-dependent RNA polymerases (18, 19) and is believed to serve as the active polymerase in both minus- and plus-strand replication complexes (2, 13, 29, 51). Mutations in the nsP4 region can result in *ts* synthesis of all three viral RNAs (13), *ts* resumption of minus-strand synthesis (43, 45), and *ts* defects which are host cell dependent (mosquito versus vertebrate) (25).

In contrast, there exist relatively few data on the role of nsP3 and nsP3-containing polyproteins in SIN-specific RNA synthesis. Unlike the nsP1, nsP2, and nsP4 regions, which show extensive homology with nonstructural proteins from other positive-strand virus families, including plant viruses (1, 18), only a short sequence near the N terminus of nsP3 shows weak homology to rubella virus, another togavirus, and avian infectious bronchitis virus, a coronavirus (7, 10). The alphavirus nsP3 region consists of a conserved N-terminal portion and a nonconserved C-terminal portion, which is highly variable in sequence and length among alphaviruses (55) and is mostly dispensable for SIN replication in vertebrate cells (24). nsP3 and some nsP3-containing polyproteins are phosphorylated in vivo, resulting in the production of a number of electrophoretically distinct forms (31). The role of these phosphorylated species in SIN RNA replication, if any, is unknown. Interestingly, nsP3 can also be phosphorylated in vitro by an associated serine/threonine-specific protein kinase which may be the same enzyme responsible for nsP3 phosphorylation in virus-infected cells (31).

Although characterization of SIN RNA$^-$ *ts* mutants in the nsP3 region could provide insight into its function, only one RNA$^-$ lesion has been mapped to nsP3 (14). This mutation was derived from the double mutant *ts*7 and produces a virus with a leaky *ts* phenotype. In an attempt to further characterize the role of the nsP3 region in viral RNA synthesis, we report the isolation and characterization of a number of mutants derived from libraries of random linker insertion mutations in the SIN nsP3 region. The RNA phenotypes of some of these mutants suggest that nsP3 or nsP3-containing polyproteins play an important role in the synthesis of both minus-strand and subgenomic plus-strand RNAs.

MATERIALS AND METHODS

Cell cultures, virus stocks, and plaque assay. Secondary chicken embryo fibroblasts (CEF) were propagated as previously described (38). All virus stocks were generated either by DEAE-dextran-mediated transfection of CEF with RNA transcribed in vitro from the mutant cDNAs as templates (40) or by the isolation of virus from plaques on CEF monolayers and subsequent passaging in CEF. Infections and plaque assays were done as previously described, using virus diluted in phosphate-buffered saline (PBS) containing 1% fetal calf serum (38). pToto:*ts*11A1, pToto:*ts*17B1, pToto:*ts*18B1, and pToto:*ts*110C2 cDNAs used for in vitro transcription were kindly provided by Y. S. Hahn (13, 14).

Plasmid construction and site-directed mutagenesis. All recombinant DNA manipulations were done essentially as described elsewhere (34) with reagents from commercial sources. Numbering refers to the nucleotide positions in the SIN genome RNA (or cDNA) sequence (57). To construct the parental clone with the unique *Mlu*I and *Xba*I restriction sites (Fig. 1) used for the generation of the nsP3 random insertion libraries, the *Nhe*I (3437)-*Eco*RI (5392) fragment from the nsP3 deletion mutant pΔ14 (24) was subcloned into the phagemid vector pH2J2 (kindly provided by C. S. Hahn) to

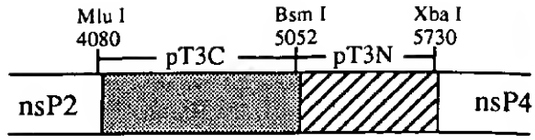

FIG. 1. SIN nsP3 conserved- and nonconserved-region linker insertion libraries. The diagram illustrates the regions of the SIN genome represented in the two random insertion libraries, pT3C and pT3N. The *Mlu*I, *Xba*I, and *Bsm*I sites used in the division of the original library into the two libraries are shown, with the position of each site in the full-length SIN cDNA sequence indicated. The conserved (shaded box) and nonconserved (hatched box) regions are indicated.

create the phagemid p3.14. Single-stranded DNA containing uracil was generated (21) from p3.14 and used for oligonucleotide-directed mutagenesis to create a unique *Mlu*I site near the 3′ end of the nsP2 gene and a unique *Xba*I site near the 3′ end of nsP3 to create the plasmid p3.14MX. The substitutions were A to G (nucleotide [nt] 4082), A to C (nt 4083), and A to T (nt 4085) to create the *Mlu*I site and A to T (nt 5730), G to C (nt 5731), C to T (nt 5732), and G to A (nt 5735) to create the *Xba*I site. A full-length nsP3-coding region was generated by subcloning the *Bst*XI (4168)-*Esp*I (5600) fragment of SIN cDNA clone pToto1101 into the *Bst*XI-*Esp*I sites of p3.14MX to produce the plasmid p3MX. The *Pst*I fragment containing nsP3 from p3MX was subcloned into the corresponding *Pst*I sites of pMT21-1101(BA), a vector containing the *Bgl*II (2288)-*Aat*II (7995) fragment of pToto1101, to create pMT21-1101(BA)MX. The *Cla*I (2712)-*Hpa*I (6917) fragment in pToto1101 was replaced with the corresponding *Hpa*I-*Cla*I fragment from pMT21-1101(BA)MX to produce the full-length parental clone for mutagenesis, called pToto1106. With this strategy, the *Pst*I (3949)-*Bst*XI (4168) and *Esp*I (5600)-*Pst*I (5820) regions were the only sequences in pToto1106 whose origin was from plasmids that had undergone site-directed mutagenesis. The nucleotide sequences of these two regions were verified by dideoxy sequencing and were identical to that of pToto1101 except for the silent mutations introduced to create the *Mlu*I and *Xba*I restriction sites.

Random insertion mutagenesis. Supercoiled monomer p3MX DNA, purified from the *recA Escherichia coli* strain WM1100 by banding twice in cesium chloride gradients, was treated with DNase I in 20 mM Tris (pH 7.5)–1.5 mM $MnCl_2$–0.02 mg of gelatin per ml to produce randomly linearized full-length fragments. DNase I-treated p3MX DNA was repaired with T4 DNA polymerase to fill in 5′ overhanging ends or remove 3′ overhanging ends and then dephosphorylated with calf intestinal alkaline phosphatase. Randomly linearized p3MX DNA molecules were isolated after separation by electrophoresis on a low-melting-point agarose gel and ligated with a phosphorylated *Sph*I 12-mer linker (5′-GCAT GCGCATGC-3′). The *Sph*I recognition sequence is not found in either p3MX or pToto1106, which allowed selection of mutant plasmids containing the inserted linker. The ligation products were used to transform MC1061 by electroporation, creating the initial library of random insertion mutations. The *Mlu*I-*Xba*I fragment from the original library was subcloned into p3MX, and this library was selected once for the presence of the *Sph*I restriction site by digestion with *Sph*I, isolation and intramolecular ligation of the linearized molecules, and transformation of MC1061 by electroporation to produce the library designated p3RSS. p3RSS was then split into two libraries by subcloning the *Mlu*I (4080)-*Bsm*I (5052) and *Bsm*I (5052)-*Xba*I

(5730) regions from p3RSS into p3MX, and each library was selected once for the presence of the *Sph*I site to produce the two libraries p3MBS and p3BXS. The *Mlu*I (4080)-*Xba*I (5730) region from the p3MBS and p3BXS libraries was cloned into the corresponding region in pToto1106 and selected once for the *Sph*I site to produce the final nsP3 conserved-region mutant library, pT3C, and the nonconserved-region mutant library, pT3N (Fig. 1).

Cloning of random mutations. Tissue culture wells (22-mm diameter) containing CEF were infected with 100 μl of the virus stocks (undefined multiplicity of infection [MOI]) of the 13 isolates from the pT3C library for 1 h at room temperature. After 7 h at 30°C, total cellular RNA was prepared from the infected cells by lysis of the cells with 200 μl of 2% sodium dodecyl sulfate (SDS) containing 50 μg of proteinase K per ml, extraction with phenol-chloroform, and precipitation with sodium acetate and ethanol. First-strand cDNA synthesis was performed by reverse transcription (11) of viral plus strands by using a minus-sense primer followed by symmetric PCR amplification (41) with primers either flanking or internal to the nsP3 conserved-region coding sequence. The approximate locations of the inserted *Sph*I linkers in the PCR-amplified DNA were determined by restriction analysis. Mutant cDNA fragments in which the *Sph*I linker was between the *Mlu*I (4080) and *Avr*II (4280) sites (unique in pToto1106) were digested with these two enzymes, and the resulting fragment containing the insertion was cloned directly into pToto1106. cDNA fragments for the remaining mutants were subcloned first into p3MX by using convenient restriction sites and then into pToto1106 by using the *Mlu*I and *Xba*I sites. Subcloned regions obtained by RNA PCR were sequenced completely by the dideoxy method (42).

RNA analysis of conserved-region mutants. CEF in two sets of 22-mm-diameter tissue culture wells were infected at an MOI of 20 for 1 h at 4°C. The virus inoculum was removed from the cells, and medium (prewarmed to either 30 or 40°C) containing 1 μg of dactinomycin per ml was added and the cells were incubated at 30 or 40°C. At 3.5 h postinfection, the medium from each monolayer was replaced with medium (prewarmed to either 30 or 40°C) containing 1 μg of dactinomycin per ml and 20 μCi of [^{3}H]uridine per ml. Incubation of the cells was continued at 30 or 40°C for an additional 3 h, at which time the monolayers were washed once with ice-cold PBS and then lysed with 200 μl of 1% Triton X-100. A 30-μl volume of each lysate was precipitated with trichloroacetic acid (TCA) (25), and the amount of radioactivity incorporated into total viral RNA was determined in scintillation fluid.

For measurement of genomic and subgenomic RNA synthesis, radiolabeled cells (as described above) were washed once with ice-cold PBS and lysed with 200 μl of 5% SDS containing 50 μg of proteinase K per ml. One-twentieth of each lysate was separated by agarose gel electrophoresis (2), and the gel was treated for fluorography. Genomic and subgenomic RNA bands, as well as the corresponding area from a mock-infected sample, were localized by fluorography (23) and excised, and the incorporation of radioactivity into each RNA species was determined by liquid scintillation counting.

Analysis of *ts* RNA phenotypes. For analysis of *ts* effects on plus-strand synthesis late in infection, five sets of 22-mm-diameter tissue culture wells containing CEF were infected at an MOI of 25. Following adsorption for 1 h at 4°C, the virus inoculum was replaced with medium (prewarmed to 30°C) containing 1 μg of dactinomycin per ml and the cultures were incubated at 30°C for the times specified below. Three of the five sets of infected cells were labeled for 1 h at 30°C with medium (prewarmed to 30°C) containing 1 μg of dactinomycin per ml and 50 μCi of [^{3}H]uridine per ml beginning at either 5.5, 6.5, or 7.5 h postinfection. For the remaining two sets of infected cells, the medium was replaced with medium (prewarmed to 40°C) containing 1 μg of dactinomycin per ml at 6 h postinfection and the cells were incubated at 40°C. The two sets of cells shifted to 40°C were labeled for 1 h at 40°C with medium (prewarmed to 40°C) containing 1 μg of dactinomycin per ml and 50 μCi of [^{3}H]uridine per ml beginning at either 6.5 or 7.5 h postinfection. Following labeling, the cells were washed once with ice-cold PBS and each monolayer was lysed with 200 μl of 1% Triton X-100. A 30-μl volume of each sample was precipitated with TCA and radioactivity was counted as described above.

For minus-strand analysis, five sets of CEF monolayers in 35-mm-diameter tissue culture wells were infected at an MOI of 25. After adsorption for 1 h at 4°C, the virus inoculum was replaced with medium (prewarmed to 30°C) containing 1 μg of dactinomycin per ml and the cultures were incubated at 30°C for the times specified below. Three of the five sets of infected cells were maintained at 30°C and labeled for 45 min with 250 μCi of [^{3}H]uridine per ml in medium (prewarmed to 30°C) containing 0.2% bovine serum albumin and 1 μg of dactinomycin per ml beginning at 2, 3, and 3 h 45 min postinfection. At 2 h 30 min postinfection, the medium of the remaining two sets of cells was replaced with medium (prewarmed to 40°C) containing 1 μg of dactinomycin per ml and the cells were incubated at 40°C. The cells shifted to 40°C were labeled for 45 min beginning at either 3 h or 3 h 45 min postinfection with labeling medium prewarmed to 40°C. After the labeling, monolayers were washed once with ice-cold PBS and RNA was isolated with RNAzol (Tel-Test, Inc.), precipitated with 2-propanol, washed once with 80% ethanol, and resuspended in 15 μl of H_2O. The A_{260} was determined for each sample and used to equalize input RNAs. Radioactive label incorporated into total viral RNA was determined by liquid scintillation counting of TCA-precipitated samples. Radioactive label incorporated into minus-strand RNA was determined by RNase protection (37). Typically, 15 to 20% of the RNA recovered from a 35-mm-diameter tissue culture plate was used for minus-strand analysis. Equal amounts of each RNA sample were diluted at least 1:10 (total volume, 30 μl) with hybridization buffer containing 80% deionized formamide, 40 mM PIPES [piperazine-*N*,*N*′-bis(2-ethanesulfonic acid)] (pH 6.4), 400 mM NaCl, and 1 mM EDTA, denatured by incubation at 95°C for 5 min, vortexed, and heated at 95°C for an additional 5 min. Samples were cooled slowly to 55°C (approximately 2 h) and allowed to anneal for a minimum of 12 h at 55°C. A 300-μl volume of an RNase cocktail (300 mM NaCl, 10 mM Tris [pH 7.5], 5 mM EDTA, 15 μg of RNase A per ml, and 350 U of RNase T1 per ml) was added, and the mixture was incubated for 1 h at room temperature. A 10-μl volume of 10% SDS and 10 μl of proteinase K (10 mg/ml) were then added to each sample, and incubation was continued for 15 min at 37°C. After addition of 10 μg of *Saccharomyces cerevisiae* tRNA, samples were extracted with phenol and precipitated with sodium acetate and ethanol. RNA pellets were washed once with 80% ethanol and resuspended in 30 μl of hybridization buffer containing 10 μg of Toto1101 RNA produced by in vitro transcription (40). The samples then underwent a second round of denaturation, annealing, and RNase treatment exactly as described before except that the final RNA pellets were resuspended in 30 μl of H_2O. Resuspended RNAs were precipitated with TCA, and the counts per minute were determined by liquid scintillation counting. For each sample, the amount of radioactive label incorporated into minus-strand RNA is the amount of pro-

ected counts per minute minus the protected counts per minute in the mock-infected control.

Complementation analyses. CEF in 22-mm-diameter tissue culture wells were infected at an MOI of 50 with a combination of two mutants (each at 50 PFU per cell) or each mutant alone (at 50 PFU per cell). After adsorption for 1 h at 40°C, the cells were washed once with medium and then incubated at 40°C in medium containing 1 μg of dactinomycin per ml. At 2 h postinfection, the monolayers were washed once with medium and incubation was continued at 40°C. At 6.5 h postinfection, the medium from each sample was collected and the yield of virus was determined by plaque assay on CEF monolayers at 30°C.

Plaque hybridization. Virus derived from the complementation assays of CR3.36 and Toto:*ts*110C2, or CR3.39 and Toto:*ts*110C2, or the single infections of these mutants were used to infect 100-mm-diameter plates of CEF with approximately 200 PFU per plate. Following adsorption at 4°C for 1 h, plates were overlaid with medium containing agarose and incubated at 30°C. After 3 days, monolayers were stained with neutral red to determine the total number of plaques. The monolayers were then transferred to nitrocellulose filters and probed for the presence of either CR3.36 or CR3.39 plaques (33). 18-mer synthetic oligonucleotides containing the *Sph*I recognition sequence and six nucleotides of 5′- and 3′-flanking sequence corresponding to CR3.36 and CR3.39 insertion sites were used as specific hybridization probes for CR3.36 and CR3.39 plaques, respectively.

In vivo labeling and immunoprecipitation of nsP3. For the analysis of metabolically labeled nsP3, two sets of 22-mm-diameter tissue culture wells containing CEF were infected at an MOI of 10. After adsorption for 1 h at room temperature, the virus inoculum was replaced with medium (prewarmed to 30°C) and the cells were incubated at 30°C. At 4 h postinfection, one set of infected monolayers was shifted to 40°C. At 5 h postinfection, the monolayers were washed once with medium lacking Met and labeled with 20 μCi of [^{35}S]Met in medium lacking Met (prewarmed to either 30 or 40°C) containing 2% fetal calf serum. Following incubation for an additional 2 h at either 30 or 40°C, the cells were washed once with ice-cold PBS and lysed with 200 μl of 1% SDS containing 20 μg of phenylmethylsulfonyl fluoride per ml. nsP3 was immunoprecipitated from the labeled lysates (26, 33), and the products were analyzed by SDS-polyacrylamide gel electrophoresis (PAGE) (22). Gels were treated for fluorography (34), dried, and exposed to X-ray film.

RESULTS

Random mutagenesis of SIN nsP3. The method chosen for creating mutations in the nsP3 region was random cleavage using DNase I followed by insertion of an *Sph*I linker. To select for mutations confined primarily to the nsP3-coding region and to facilitate subcloning steps, two novel restriction enzyme sites were created near the 5′ and 3′ boundaries of the nsP3-coding region. Silent changes were used to create a unique *Mlu*I (4080) site near the 3′ end of the nsP2-coding region and a unique *Xba*I (5730) site near the 3′ end of the nsP3-coding region. The location of these restriction sites was such that the random insertion mutation library would include mutations in the 3′-terminal 15 nt of the nsP2-coding region and would lack mutations in the 3′-terminal 18 nt of the nsP3 gene. The parental SIN cDNA clone containing these two new restriction sites was designated pToto1106 and is isogenic with pToto1101 (40) except for the seven silent nucleotide changes used to create the *Mlu*I and *Xba*I sites. No differences in plaque morphology, growth rate, and genomic or subgenomic RNA synthesis were found at either 30, 37, or 40°C between Toto1101, which has often been used as the parental virus for the examination of SIN mutants (13, 14, 25, 35), and Toto1106 (data not shown).

Monomer supercoiled DNA of the nsP3 shuttle plasmid p3MX was used for random mutagenesis to produce an initial library of 720,000 clones. Approximately 25% of the DNA prepared from the original library could be linearized by *Sph*I, hence the original library contained ~180,000 *Sph*I-positive clones. The p3MX plasmid contains 4,697 bp, which results in a library complexity estimated at 38 independent insertion mutations per base pair. The degree of complexity of the original library was maintained throughout all subsequent cloning steps. The *Bsm*I site near the junction of the conserved and nonconserved regions was used to divide the nsP3 insertion library into two libraries: one for the conserved region (pT3C) and a second for the nonconserved region (pT3N) (Fig. 1).

Isolation and initial characterization of SIN nsP3 mutants. Plasmid DNA prepared from the pT3C and pT3N libraries was linearized with *Xho*I and transcribed with SP6 RNA polymerase, and the resulting RNA was used to transfect CEF (40). Transcript RNA from these libraries was expected to have a lower specific infectivity (PFU per nanogram of RNA) than Toto1106 RNA, for two reasons. First, because of the repair of 5′ or 3′ protruding ends, two-thirds of the insertion mutations should be out of frame and therefore lethal. Second, even for in-frame insertions, at least some mutations were expected to be lethal for plaque formation. Compared with that of Toto1106 RNA, the specific infectivity (at 30 or 40°C) for the pT3C library was 10- to 20-fold lower while that for the pT3N library was only two- to fourfold lower. Plaque size heterogeneity was especially evident in the pT3C library. As predicted, these observations suggested that the conserved region was much more sensitive to mutagenesis than the nonconserved region.

Both small and large plaques, 126 from the pT3C library and 23 from the pT3N library, were isolated from transfected monolayers incubated at 30°C. Virus stocks were generated at 30°C and the titers were determined at both 30 and 40°C to screen for mutants that either were *ts* for plaque formation or displayed reproducible differences in plaque phenotype compared with that of the parental virus. Thirty-seven of the 126 isolates from the pT3C library were significantly *ts*, with reductions in plaquing efficiency ranging from 10-fold to more than 1,000-fold compared with that of Toto1106. In addition, some isolates from the pT3C library, although not *ts*, demonstrated significant differences in plaque morphology compared with that of Toto1106 at 30 and/or 40°C. In contrast, only two of the 23 isolates from the pT3N library were found to be slightly *ts* (10- to 15-fold reductions compared with Toto1106). Given the high specific infectivity of the pT3N library at both 30 and 40°C and our inability to identify highly *ts* mutants in initial 30°C plaque isolates, we have not characterized mutants derived from the pT3N library further.

Thirteen isolates from the pT3C library, those which were strongly *ts* and some which exhibited significant differences in plaque morphology, were chosen for further characterization. The regions containing the linker insertion mutations were amplified by reverse transcriptase PCR and cloned into the pToto1106 background and are designated CR3.31 to CR3.43. Appropriate regions were sequenced, and the nucleotide and deduced amino acid sequences at the insertion sites are shown in Fig. 2A. The mutations in CR3.34, CR3.36, CR3.37, CR3.38, CR3.39, CR3.41, CR3.42, and CR3.43 included the *Sph*I

A

Mutant	Nucleotide Sequence	Amino Acid Sequence
CR3.31	4113 [GCATGC] 4120 4200 [A] 4202	5 [MQ] 8 33 [Y] 35
CR3.32	4160 [GCATGC] 4170	20 [AC] 24
CR3.33	4279 [GCATGC] 4286	59 [WHA] 63
CR3.34	4857 [GCATGC] 4855	252 [RMH] 253
CR3.35	4265 [GCATGC] 4266	55 [AC] 56
CR3.36	4275 [GCATGC] 4264	58 [GMPRMT] 59
CR3.37	4336 [GCATGC] 4328	79 [HAPEA] 80
CR3.38	4333 [GCATGC] 4328	78 [HAPE] 79
CR3.39	4778 [GCATGC] 4767	226 [ACNDQE] 227
CR3.40	4199 [GCATGC] 4200	33 [AC] 34
CR3.41	4773 [GCATGC] 4762	224 [RMLPND] 225
CR3.42	4336 [GCATGC] 4328	79 [HAPEA] 80
CR3.43	4933 [GCATGC] 4931	277 [RHA] 278

B

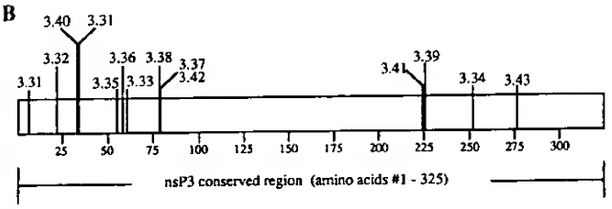

FIG. 2. Description and location of nsP3 mutations. (A) Nucleotide sequence positions (in the SIN cDNA sequence) flanking the various *Sph*I linker insertion mutations. The corresponding amino acid sequences are given, with the numbers indicating the positions of the parental nsP3 residues flanking the insert. (B) Diagram of the conserved region of nsP3 illustrating the distribution of mutations (CR prefix omitted) cloned from the random insertion library pT3C.

6-base recognition sequence plus duplications in the flanking sequence of either 3, 6, 9, or 12 bases. CR3.31, CR3.32, and CR3.33 had deletions of either 6 or 9 flanking bases, in addition to the *Sph*I 6-mer insertion. CR3.35 and CR3.40 were the only mutants in which the *Sph*I linker was inserted without duplication or deletion of flanking sequences. Duplication or deletion of the flanking wild-type sequences at the insertion points presumably arose during repair of DNase I-linearized DNA containing 5′ or 3′ overhanging ends with T4 DNA polymerase. In all cases, the original *Sph*I 12-mer linker used for mutagenesis had been reduced to a 6-mer, presumably during the multiple *Sph*I selections used to construct the mutant libraries. CR3.31 contained a second mutation which resulted in the conversion of Cys-34, an amino acid which is conserved among all alphavirus nsP3 sequences reported, to Tyr. The origin of this additional mutation is unknown, and whether the phenotype of CR3.31 is a result of one of these mutations by itself or a combination of both has not been determined. The majority of the mutations clustered in the N-terminal one-fourth of the conserved region, with the remaining mutations located in the C-terminal one-third. The insertion mutations in CR3.37 and CR3.42 were identical and similar to that of mutant CR3.38, which contained a net insertion of four amino acids instead of five. The CR3.32 mutation was located near the N terminus of nsP3 in the sequence which shows some homology with rubella virus and avian infectious bronchitis virus (7, 10).

Mutant virus stocks used in subsequent experiments were generated by transfection of CEF with RNA transcribed from the mutant cDNA clones. The titers of the resulting virus stocks were determined at 30 and 40°C (Table 1). All of the mutants grew to relatively high titers (>6×10^8 PFU/ml at 30°C) except for CR3.31, which only reached a titer of 3×10^7 PFU/ml at 30°C. A few of the mutant virus stocks derived from

TABLE 1. Efficiency of plaque formation of nsP3 mutants

Virus	EOP[a]	Plaque morphology[b]	
		30°C	40°C
Toto1106	1.0	L	L
CR3.31	1.1×10^{-4}	S	S + L
CR3.32	1.0	L	L
CR3.33	$<1.8 \times 10^{-3}$	M	No plaques
CR3.34	9.1×10^{-1}	M	S + M
CR3.35	3.8×10^{-7}	M	S
CR3.36	$<1.9 \times 10^{-7}$	M	No plaques
CR3.37	1.9×10^{-4}	M	S, M, + L
CR3.38	4.0×10^{-2}	M	S + L
CR3.39	$<1.9 \times 10^{-7}$	M	No plaques
CR3.40	8.3×10^{-1}	M	L
CR3.41	$<1.5 \times 10^{-7}$	M	No plaques
CR3.43	1.5×10^{-1}	S	S

[a] EOP, efficiency of plaque formation, determined as the titer of each virus at 40°C divided by its titer at 30°C.
[b] Relative size of plaques (L, large; M, medium; S, small).

cDNA were not markedly *ts* (CR3.32 and CR3.40), suggesting that the original phenotype had been lost upon cloning (either because the *ts* lesion was unlinked to the *Sph*I linker insertion or because a contaminating non-*ts* insertion mutant was cloned). In any case, mutants CR3.35, CR3.36, CR3.39, and CR3.41 were highly *ts*. Mutants CR3.31, CR3.33, CR3.37, and CR3.38 displayed an intermediate level of temperature sensitivity, and all four exhibited plaque size heterogeneity at 40°C. Although CR3.34 and CR3.43 did not exhibit significant temperature sensitivity, they were distinguishable from Toto1106 by their smaller-plaque phenotype. Although all plaques were smaller than Toto1106 plaques, the CR3.34 stock demonstrated obvious plaque heterogeneity.

RNA synthesis phenotype of nsP3 conserved region mutants. Ten of the cloned mutants were tested for their ability to synthesize RNA at 30 and 40°C (Table 2). CR3.31 was not tested since a high-titer virus stock could not be generated, CR3.40 was not significantly different from the parental virus to warrant its inclusion, and CR3.42 was not tested since it was identical to CR3.37. Although CR3.32 did not display any obvious differences with the parental virus in terms of efficiency of plaque formation or plaque morphology, it was included because the mutation was located in a conserved region of nsP3 with apparent homology to rubella virus and avian infectious bronchitis virus. The level of RNA accumulated at 30°C ranged from 0.5 to 1.5 times the level of Toto1106. CR3.37 and CR3.38, containing similar insertions, synthesized somewhat higher levels of total viral RNA at 30°C. CR3.32, CR3.34, CR3.35, CR3.36, and CR3.39 accumulated somewhat less RNA than the parental virus at 30°C. At 40°C, all of the mutants accumulated significantly less RNA than Toto1106, although for CR3.32, RNA synthesis was similarly impaired at 30°C. RNA synthesis was undetectable for mutants CR3.35, CR3.36, CR3.39, and CR3.41. As might be expected for mutations in the nonstructural protein-coding region, all mutants *ts* for plaque formation were also *ts* for RNA synthesis. However, the relative levels of RNA accumulation at 40°C did not directly correlate with degree of temperature sensitivity as assayed by plaque formation. For instance, CR3.43, while not as *ts* as CR3.33 or CR3.38 for plaque formation, accumulated less RNA at the nonpermissive temperature.

Lysates of [^{3}H]uridine-labeled infected cells were also run on an agarose gel, and the incorporation of label specifically into viral genomic and subgenomic RNAs was determined

TABLE 2. Synthesis of viral RNA at 30 and 40°C[a]

Mutant	RNA synthesis		Molar ratio of 49S:26S RNA	
	30°C	40°C	30°C	40°C
Toto1106	1.0	1.0	0.1	0.3
CR3.32	0.5	0.5	0.1	0.3
CR3.33	1.1	0.4	0.1	0.2
CR3.34	0.7	0.4	1.7	3.4
CR3.35	0.5	0.0	0.1	ND[b]
CR3.36	0.6	0.0	0.1	ND
CR3.37	1.4	0.1	0.1	0.2
CR3.38	1.5	0.2	0.1	0.2
CR3.39	0.5	0.0	0.1	ND
CR3.41	0.9	0.0	0.1	ND
CR3.43	1.2	0.1	0.1	0.2

[a] CEF infected with the indicated viruses were labeled with [^{3}H]uridine 3.5 to 6.5 h postinfection in the presence of dactinomycin at the indicated temperatures. Incorporation was determined by TCA precipitation and is reported relative to the Toto1106 value at the same temperature. To determine the molar ratio of 49S/26S RNA, these species were separated by gel electrophoresis (Fig. 3), localized by fluorography, and excised and radioactivity was counted.
[b] ND, not determined.

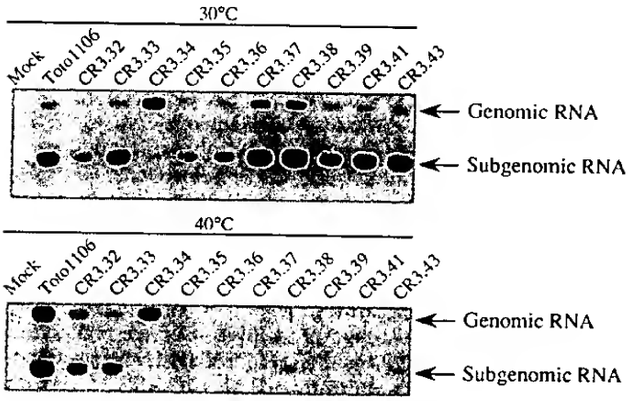

FIG. 3. Synthesis of genomic and subgenomic viral RNAs. RNA labeled with [^{3}H]uridine 3.5 to 6.5 h postinfection in the presence of dactinomycin at the indicated temperature was resolved under nondenaturing conditions by gel electrophoresis on 1% agarose gels.

(Table 2; Fig. 3). Under these lysis and electrophoresis conditions, released plus strands resolve from replicative intermediates (which contain minus strands and nascent plus strands) which migrate more slowly (2). The molar ratio of genomic (49S) to subgenomic (26S) RNA for each mutant at 30 and 40°C was determined. Only CR3.34 exhibited a significant difference in the ratio at either temperature. Even though the molar ratio of genomic to subgenomic RNA synthesis varies during a normal infection, the ratios determined for CR3.34 were significantly higher than what is found for the parental virus at any time postinfection. Relative to Toto1106, CR3.34 accumulated significantly more genomic RNA at 30°C and slightly less at 40°C. At both temperatures, CR3.34 exhibited dramatically reduced subgenomic RNA accumulation. Since the CR3.34 virus stock used in these experiments demonstrated obvious heterogeneity in plaque size at 40°C, indicating the possible presence of revertants, a first-cycle analysis of plus-strand RNA synthesis by the CR3.34 mutant was done by labeling viral RNA in CEF which had been transfected with in vitro-transcribed CR3.34 RNA. Examination of the CR3.34 first-cycle RNA on an agarose gel (data not shown) verified the dramatic defect in subgenomic RNA synthesis and accumulation.

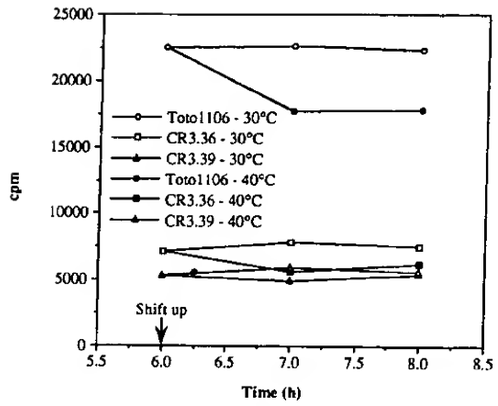

FIG. 4. Viral plus-strand synthesis late in infection. Monolayers of CEF infected with Toto1106, CR3.36, or CR3.39 were incubated and labeled with [^{3}H]uridine at 30°C at the indicated times or incubated initially at 30°C, shifted to 40°C at 6 h postinfection, and labeled at 40°C at the indicated times. Each sample was labeled for 1 h, and incorporation of label into total viral RNA was determined by TCA precipitation and liquid scintillation counting. Datum points are plotted at the midpoint of the labeling period and are the averages of three experiments.

Examination of *ts* RNA phenotype of CR3.36 and CR3.39. As mutants CR3.36 and CR3.39 were highly *ts*, experiments were conducted to determine the defect in viral RNA synthesis which led to their *ts* RNA$^-$ phenotype. At the permissive temperature, synthesis of total viral RNA and minus-strand RNA was depressed for both CR3.36 and CR3.39 compared with the parental virus. However, the time after infection at which the rate of total viral RNA synthesis reached a maximum (approximately 5 h postinfection) and the timing of the shutoff of minus-strand synthesis (maximum minus-strand synthesis at approximately 3 h postinfection and shutoff by approximately 5 h postinfection) for each mutant was similar to that of the parental virus (data not shown).

The effect of a shift to the nonpermissive temperature on plus-strand synthesis was examined late in infection, after minus-strand synthesis was shut off. Since minus-strand synthesis had already decreased to a minimum level by the time of the shift-up, any effects of the shift to the nonpermissive temperature on plus-strand synthesis should be representative primarily of a *ts* effect on plus-strand synthesis and not a secondary effect from a *ts* effect on minus-strand synthesis. For CR3.36, CR3.39, and Toto1106, plus-strand synthesis decreased slightly upon shift to the nonpermissive temperature (Fig. 4). The percent reduction in plus-strand synthesis for both mutants was similar to that for Toto1106, indicating that neither mutation has a *ts* effect on plus-strand synthesis.

The experiment whose results are shown in Fig. 5 examined the rate of synthesis of both total viral RNA and minus-strand RNA at the permissive temperature and after a shift to the nonpermissive temperature, early in infection when viral minus-strand RNA synthesis is actively occurring. Toto:*ts*11A1 (14, 46, 61), a previously isolated *ts* SIN mutant defective in minus-strand synthesis, was included for comparison. The results obtained for CR3.36, CR3.39, and Toto:*ts*11A1 were similar, with all three mutants exhibiting continued synthesis of total viral RNA upon shift-up to 40°C, whereas minus-strand synthesis rapidly ceased. Upon shift to 40°C, total viral RNA synthesis for Toto1106 increased significantly, compared with that at 30°C, while the rate of synthesis of total viral RNA for all three mutants remained approximately the same as it was at

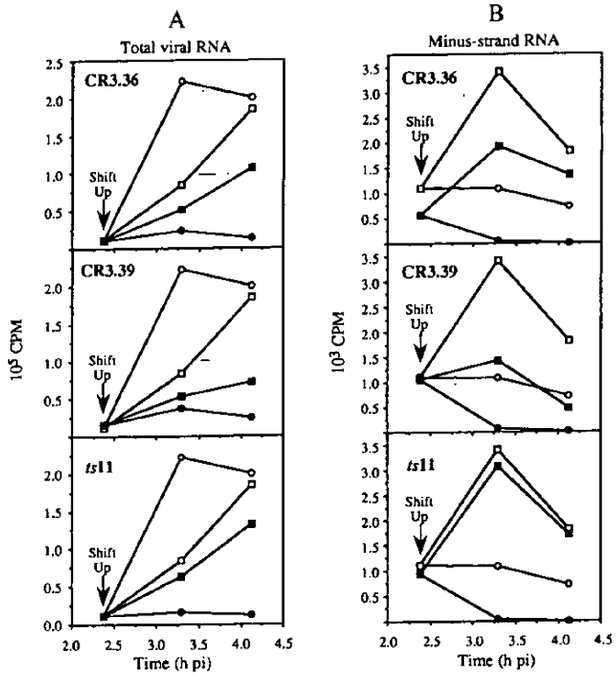

FIG. 5. Analysis of RNA phenotypes early in infection. Monolayers of CEF infected with Toto1106, CR3.36, CR3.39, or Toto:*ts*11A1 were incubated and labeled with [^{3}H]uridine at 30°C at the indicated times or incubated initially at 30°C, shifted to 40°C at 2 h 20 min postinfection, and labeled at 40°C at the indicated times. Datum points are plotted at the midpoint of each 45-min labeling period. (A) Incorporation of radioactive label into total viral RNA. (B) Incorporation of radioactive label into viral minus strands. For comparison, the data for Toto1106 are reproduced in each of the panels. Values for Toto1106 at 30°C and after shift-up to 40°C (open squares and circles, respectively) and corresponding values for the indicated mutants (filled squares and circles) are shown. The time of shift to 40°C is indicated by arrows. It should be noted that the *ts*11 lesion was analyzed in the Toto1101, rather than the Toto1106, genetic background. This difference is unlikely to have affected the *ts*11 phenotype since these parental strains differ by only seven silent changes and have similar growth and RNA accumulation phenotypes (14) (data not shown).

the time of the shift. These results can at least be partially explained by the lack of minus-strand synthesis after shift-up for the three mutants, resulting in no additional templates for increased plus-strand synthesis. In contrast, the parental virus continued to synthesize minus strands at 40°C which could serve as templates to increase the level of plus-strand synthesis. Viral RNA, labeled at 30°C or after the shift to 40°C, was analyzed by gel electrophoresis, and no obvious differences in the ratio of genomic to subgenomic RNA synthesized were observed (data not shown). Therefore, it appears that the *ts* defect in RNA replication for the mutants CR3.36 and CR3.39 is in minus-strand RNA synthesis. These experiments do not distinguish between initiation versus elongation defects.

Complementation of CR3.36 and CR3.39 with RNA$^-$ *ts* mutants. The ability of mutants CR3.36 and CR3.39 to complement each other, and representatives from the four established RNA$^-$ complementation groups of SIN, was examined in a standard mixed infection at the nonpermissive temperature (Table 3). The representative *ts* mutants from complementation groups A, B, F, and G were Toto:*ts*17B1, Toto:*ts*11A1, Toto:*ts*110C2, and Toto:*ts*18B1, respectively (13, 14). CR3.39 complemented mutants from all four groups, thus

TABLE 3. Complementation analysis of CR3.36 and CR3.39

Mutant	Complementation index[a]				
	Group A (*ts*17)	Group B (*ts*11)	Group F (*ts*110)	Group G (*ts*18)	CR3.39
CR3.36	1.7	27	209	6.4	1.0
CR3.39	24	124	363	11	

[a] Yield of virus in a mixed infection at 40°C divided by the sum of the yields of each mutant alone at 40°C. Values are the average of two experiments.

establishing a fifth complementation group among the nonstructural proteins. CR3.36 was able to complement mutants from groups B, G, and F, although none as well as CR3.39; however, complementation of CR3.36 with Toto:*ts*17B1 could not be detected. Both CR3.36 and CR3.39 complemented best with Toto:*ts*110C2. This is consistent with previous observations that complementation is often most efficient with group F mutants. The relatively low complementation value observed with Toto:*ts*18B1 was at least partially due to the leakiness of this mutant and the resulting high background at the nonpermissive temperature. Mutants CR3.36 and CR3.39 were unable to complement each other. Due to leakiness or the presence of revertants in our stock, we were unable to conduct complementation analyses with Toto:*ts*7B5, which contains a *ts* lesion in nsP3.

CR3.36 and CR3.39 defects are not *cis* acting. The experiments reported thus far do not formally exclude the possibility that the minus-strand lesions in CR3.36 and CR3.39 result from disruption of an essential *cis*-acting RNA element rather than defective nsP3-containing translation products. In the former case, CR3.36- and CR3.39-containing virions should not be amplified during complementation at the nonpermissive temperature. This possibility was tested by assaying the virus released during complementation between Toto:*ts*110C2 and CR3.36 or CR3.39 (data not shown). As assayed by plaque hybridization, coinfection of CR3.36 and Toto:*ts*110C2 at 40°C led to a 100-fold amplification of CR3.36 compared with the yield of CR3.36 alone at 40°C. Similarly, coinfection of CR3.39 and Toto:*ts*110C2 resulted in nearly 10,000-fold amplification of CR3.39 at the nonpermissive temperature. The difference in the degree of amplification between the two nsP3 mutants resulted primarily from the higher background levels of CR3.36 virus production at 40°C compared with those of CR3.39. These data showed that increased replication of the CR3.36 and CR3.39 genomes occurred during complementation and indicate that the *ts* defect is most likely a defect in nsP3 or nsP3-containing polyproteins and not a defect in a *cis*-acting RNA element important in minus-strand synthesis.

nsP3-specific polypeptides in infected cells. A subset of the mutants, selected on the basis of RNA phenotype, was selected for protein analysis. CR3.34 overproduced genomic RNA and underproduced subgenomic RNA, CR3.36 and CR3.39 were dramatically *ts* for minus-strand synthesis at 40°C, and CR3.37 reproducibly synthesized more RNA than the Toto1106 parent at 30°C. nsP3 and nsP3-containing polyproteins labeled at 30 or 40°C were immunoprecipitated and analyzed by SDS-PAGE (Fig. 6). For all mutants, nsP3 was observed at both 30 and 40°C, indicating that the observed RNA phenotypes were not a result of the inability of nsP3 to be cleaved from the polyprotein precursor or the instability of nsP3 at either temperature. At 30°C, nsP3 of both CR3.36 and CR3.37 appeared similar to that of the parental virus in both the level and the pattern of phosphorylated forms. However, at the nonpermissive temperature, nsP3 of CR3.36 and CR3.37 was

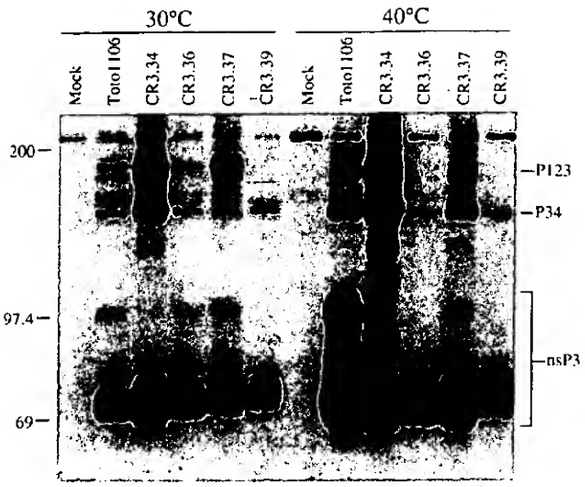

FIG. 6. Immunoprecipitation of metabolically labeled nsP3 synthesized at 30 and 40°C. Two sets of CEF monolayers were infected with Toto1106, CR3.34, CR3.36, CR3.37, or CR3.39 and incubated at 30°C. At 4 h postinfection, one set of cells was shifted to 40°C. All cells were labeled with [^{35}S]Met from 5 to 7 h postinfection, and nsP3 was immunoprecipitated from the cell lysates and analyzed by SDS-PAGE. Molecular weight markers (in kilodaltons) are indicated on the left, and the different nsP3-containing species are indicated on the right.

not converted to the slower-mobility phosphorylated forms with the efficiency of the parental nsP3. CR3.37 accumulated significantly more P123 than the parental virus at 30 and 40°C but to a lesser extent at 40°C. At both temperatures, CR3.34 overproduced nsP3, P34, and P123 relative to the parental virus, but the relative amounts of these proteins were similar, indicating that processing at the 2/3 and 3/4 cleavage sites was not affected. CR3.34 nsP3 was not converted efficiently to more slowly migrating phosphorylated forms (especially at 40°C), but some minor lower-mobility forms were observed. CR3.39 exhibited slightly altered mobility of its fastest-migrating form at both 30 and 40°C, and little, if any, was converted to the more slowly migrating forms at either temperature. Although differences in phosphorylation were obvious, there was no correlation between the extent of nsP3 phosphorylation and RNA phenotype. Since the responsible kinase and the acceptor sites have not been defined, the mechanism by which these mutations affect nsP3 phosphorylation is not known.

DISCUSSION

Chemical mutagenesis of SIN has led to the isolation of a number of *ts* mutants which have been useful for studying SIN RNA replication (3, 4, 13, 14, 25, 40, 43, 45, 54, 58, 61). These analyses have revealed a paucity of mutations in the nsP3 region. In this study, we used random insertion mutagenesis to create a library of clones containing mutations in the nsP3 region. The library was further subdivided to produce two libraries of full-length clones, one for the conserved N-terminal region and another for the nonconserved C-terminal region. From the conserved-region library, a preliminary screen was used to identify potentially interesting *ts* or plaque morphology mutants, and the RNA phenotypes of some of the mutants have been characterized in detail. These analyses suggest a role for the nsP3 region in the synthesis of both viral subgenomic and minus-strand RNAs.

The phenotype of CR3.34, which showed a dramatic and specific defect in subgenomic RNA synthesis at all temperatures examined, is somewhat surprising, given previous genetic studies (14, 44) implicating nsP2 in subgenomic RNA synthesis (see below). Although the CR3.34 mutation is located in the nsP3-coding region, we cannot conclude with absolute certainty that the observed RNA phenotype is exerted at the protein level. The inserted sequence could alter the structure of the minus-strand template, leading to inefficient initiation of subgenomic RNA synthesis. This possibility seems unlikely given the distant location of the subgenomic RNA promoter element (30), the observation that the subgenomic promoter can function in a variety of different viral sequence contexts (12, 39), and the fact that other insertion mutations in the conserved region (this work) as well as large deletions and duplications in the nonconserved region (24) did not decrease the efficiency of subgenomic RNA synthesis. It seems more likely that the RNA phenotype is a result of a defect in nsP3 or nsP3-containing polyproteins.

The CR3.34 mutation is a 3-amino-acid insertion between residues 252 and 253 of nsP3 (Fig. 7). The region is conserved among the alphaviruses and contains at least one acidic amino acid within 3 amino acids of the insertion site. If a negative charge in this region is necessary for efficient subgenomic RNA initiation, this may be disrupted by the inserted amino acids, which include an arginine and a histidine residue. Another potentially interesting feature near the CR3.34 insertion site is three serines (amino acids 254 to 256), including Ser-255, which is conserved among alphaviruses. Since the phosphorylation pattern of CR3.34 nsP3 was altered, one effect of the insertion might be to block phosphorylation at one or more of these serine residues. In this scenario, the defect in subgenomic RNA synthesis might be the result of impaired phosphorylation rather than a direct effect of the inserted sequence. Using the Toto1106 genetic background, we examined the effect of single or multiple alanine substitutions for these three serine residues. While the results suggested that Ser-255 is phosphorylated, no obvious differences in nsP3 phosphorylation were detected for the Ser-254 and/or Ser-256 substitutions (data not shown). Although the serine substitutions resulted in impaired viral RNA accumulation, none of the mutants exhibited the selective CR3.34 defect in subgenomic RNA synthesis.

The mechanism by which the CR3.34 defect allows efficient minus-strand and genomic RNA accumulation but disrupts the subgenomic RNA synthesis is unknown. Of the many possibilities, previous results with mutant CR3.4 make it unlikely that this region of nsP3 interacts directly with the subgenomic promoter element (32). CR3.4 contains a deletion of nsP3 residues 219 to 273, which includes the site of the CR3.34 insertion mutation. Although the CR3.4 mutation is lethal for viral plaque formation, subgenomic RNA can be synthesized, arguing against the possibility that this region interacts directly with the promoter to initiate subgenomic RNA synthesis. Alternatively, *ts* mutations in nsP2 which result in impaired polyprotein processing (15) or substitutions at the 1/2 and 2/3 cleavage sites engineered to block processing (50) dramatically decrease the efficiency of subgenomic RNA synthesis (28). These results suggest that cleavage of P123 could alter the template specificity of the replication complex to prefer minus-strand templates, leading to efficient initiation of genomic and subgenomic plus-strand synthesis (28). Although CR3.34 does overproduce uncleaved polyproteins, the ratio of P123 to nsP3 does not appear to be significantly different from that of the parent, suggesting that this may not be the explanation for inefficient subgenomic RNA synthesis. Further, CR3.37, which exhibits a defect in P123 processing at 30°C and accumulates levels similar to those of CR3.34, does not have impaired

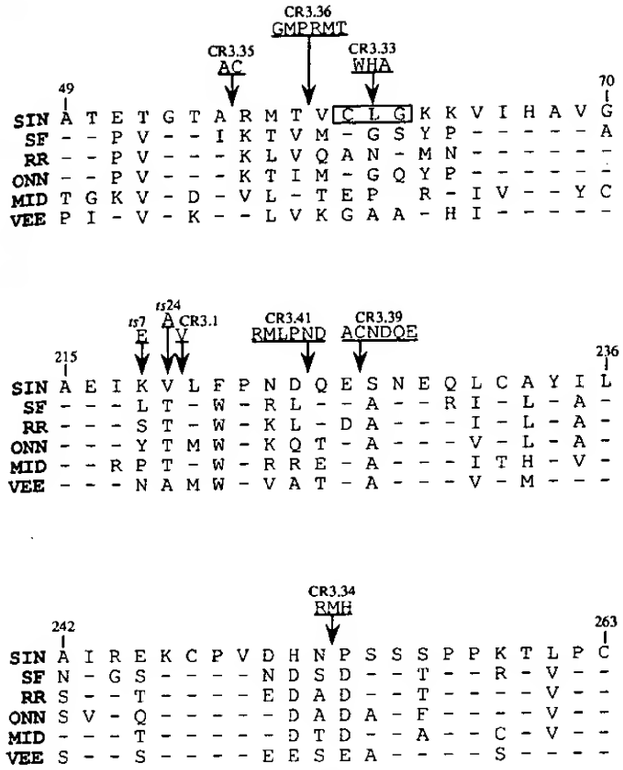

FIG. 7. Comparison of alphavirus sequences near SIN nsP3 mutations. Sequences near selected nsP3 mutations are aligned for six alphaviruses: SIN (56), Semliki Forest virus (SF) (60), Ross River virus (RR) (55), O'nyong-nyong virus (ONN) (55), Middelburg virus (MID) (56), and Venezuelan equine encephalitis virus (VEE) (20). Dashes indicate identity to the SIN sequence, and spaces indicate gaps introduced for alignment purposes. The numbers denote the first and last nsP3 residues of each region shown. The sequences and positions of the CR3.1, CR3.33, CR3.34, CR3.35, CR3.36, CR3.39, and CR3.41 insertion mutations and the *ts*7 and *ts*24 nsP3 substitution mutations (vertical arrows) and parental residues replaced with mutant amino acids (boxed residues) are indicated. The CR3.1 insertion mutation is highly deleterious for viral replication and reverts quickly (18a). Substitutions of Lys-218 with glutamic acid in *ts*7 or Val-219 with alanine in *ts*24 have no apparent effect on viral replication at either 30 or 40°C.

subgenomic RNA synthesis at this temperature. Despite cleavage at the 1/2 and 2/3 sites, the CR3.34 mutation may not allow the transcription complex to assume the conformation necessary for efficient initiation of subgenomic RNA synthesis.

This work has also shown that mutations in the nsP3 region can also result in *ts* minus-strand synthesis. Recently, the causal mutation in *ts*4, a mutant which is also defective in minus-strand synthesis, has been mapped to nsP3 (62). Since replication of CR3.36 and CR3.39 occurs during complementation with Toto:*ts*110C2, it seems likely that the defects in these mutants act at the protein level rather than via disruption of a *cis* RNA element important for minus-strand synthesis. Complementation analysis of CR3.39 has possibly established an additional RNA$^-$ complementation group, although more extensive analyses using additional conditional mutants in the nsP3 region are needed. The *ts* mutation in nsP3 derived from *ts*7 (Phe-312 to serine) has yet to be placed into a complementation group. The most interesting finding is the ability of CR3.36 and CR3.39 to complement Toto:*ts*11A1. For *ts*11, the causal mutation resides in nsP1 and results in a *ts* minus-strand defect very similar to that of CR3.36 and CR3.39. This result implies that both the nsP1 and the nsP3 regions are involved in minus-strand synthesis. This is perhaps not surprising, given recent experiments which demonstrate that uncleaved P123 and nsP4 are required for RNA replication (29) and can function in minus-strand replication complexes (29, 51). Based on several lines of evidence, a model has been proposed (29, 51) which suggests that cleavage of P123 allows a subtle conformational change which switches its template preference to minus strands and results in initiation of plus-strand genomic and, in particular, subgenomic RNA synthesis. The rate of P123 cleavage, which accelerates during infection as the concentration of *trans*-acting nsP2-containing proteinases increases, eventually results in the shutoff of minus-strand initiation. If only uncleaved P123 can function in minus-strand initiation complexes, it is difficult to explain the positive complementation results for *ts*11 and CR3.39. Rather, these results suggest that cleavage products or other processing intermediates may be able to function in the initiation of minus-strand synthesis, at least under the conditions used for complementation. A similar conclusion has been reached in studies of *ts* mutants *ts*17, *ts*24R1, and *ts*133, which can resume minus-strand synthesis upon shift to the nonpermissive temperature without new protein synthesis (43, 45).

ACKNOWLEDGMENTS

We thank our colleagues for helpful discussions during the course of this work and members of the laboratory for critical reading of the manuscript.

This work was supported by a grant from the Public Health Service (AI24134). M.W.L. was supported as a predoctoral candidate by the Division of Biology and Biomedical Sciences at Washington University.

REFERENCES

1. **Ahlquist, P., E. G. Strauss, C. M. Rice, J. H. Strauss, J. Haseloff, and D. Zimmern.** 1985. Sindbis virus proteins nsP1 and nsP2 contain homology to nonstructural proteins from several RNA plant viruses. J. Virol. **53**:536–542.
2. **Barton, D. J., S. G. Sawicki, and D. L. Sawicki.** 1988. Demonstration in vitro of temperature-sensitive elongation of RNA in Sindbis virus mutant *ts*6. J. Virol. **62**:3597–3602.
3. **Burge, B. W., and E. R. Pfefferkorn.** 1966. Complementation between temperature-sensitive mutants of Sindbis virus. Virology **30**:214–223.
4. **Burge, B. W., and E. R. Pfefferkorn.** 1966. Isolation and characterization of conditional-lethal mutants of Sindbis virus. Virology **30**:204–213.
5. **de Groot, R. J., W. R. Hardy, Y. Shirako, and J. H. Strauss.** 1990. Cleavage-site preferences of Sindbis virus polyproteins containing the nonstructural proteinase: evidence for temporal regulation of polyprotein processing in vivo. EMBO J. **9**:2631–2638.
6. **Ding, M., and M. J. Schlesinger.** 1989. Evidence that Sindbis virus nsP2 is an autoprotease which processes the virus nonstructural polyprotein. Virology **171**:280–284.
7. **Dominguez, G., C. Wang, and T. K. Frey.** 1990. Sequence of the genome RNA of rubella virus: evidence for genetic rearrangement during togavirus evolution. Virology **177**:225–238.
8. **Frolov, I., and S. Schlesinger.** 1994. Comparison of the effects of Sindbis virus and Sindbis virus replicons on host cell protein synthesis and cytopathogenicity in BHK cells. J. Virol. **68**:1721–1727.
9. **Gorbalenya, A. E., E. V. Koonin, A. P. Donchenko, and V. M. Blinov.** 1989. Two related superfamilies of putative helicases involved in replication, recombination, repair and expression of DNA and RNA genomes. Nucleic Acids Res. **17**:4713–4729.
10. **Gorbalenya, A. E., E. V. Koonin, and M. M. C. Lai.** 1991. Putative papain-related thiol proteases of positive-strand RNA viruses.

Identification of rubi- and aphthovirus proteases and delineation of a novel conserved domain associated with proteases of rubi-, alpha- and coronaviruses. FEBS Lett. **288**:201–205.

11. **Grakoui, A., R. Levis, R. Raju, H. V. Huang, and C. M. Rice.** 1989. A *cis*-acting mutation in the Sindbis virus junction region which affects subgenomic RNA synthesis. J. Virol. **63**:5216–5227.
12. **Hahn, C. S., Y. S. Hahn, T. J. Braciale, and C. M. Rice.** 1992. Infectious Sindbis virus transient expression vectors for studying antigen processing and presentation. Proc. Natl. Acad. Sci. USA **89**:2679–2683.
13. **Hahn, Y. S., A. Grakoui, C. M. Rice, E. G. Strauss, and J. H. Strauss.** 1989. Mapping of RNA$^-$ temperature-sensitive mutants of Sindbis virus: complementation group F mutants have lesions in nsP4. J. Virol. **63**:1194–1202.
14. **Hahn, Y. S., E. G. Strauss, and J. H. Strauss.** 1989. Mapping of RNA$^-$ temperature-sensitive mutants of Sindbis virus: assignment of complementation groups A, B, and G to nonstructural proteins. J. Virol. **63**:3142–3150.
15. **Hardy, W. R., Y. S. Hahn, R. J. deGroot, E. G. Strauss, and J. H. Strauss.** 1990. Synthesis and processing of the nonstructural polyproteins of several temperature-sensitive mutants of Sindbis virus. Virology **177**:199–208.
16. **Hardy, W. R., and J. H. Strauss.** 1988. Processing of the nonstructural polyproteins of Sindbis virus: study of the kinetics in vivo using monospecific antibodies. J. Virol. **62**:998–1007.
17. **Hardy, W. R., and J. H. Strauss.** 1989. Processing the nonstructural polyproteins of Sindbis virus: nonstructural proteinase is in the C-terminal half of nsP2 and functions both in *cis* and in *trans*. J. Virol. **63**:4653–4664.
18. **Haseloff, J., P. Goelet, D. Zimmern, P. Ahlquist, R. Dasgupta, and P. Kaesberg.** 1984. Striking similarities in amino acid sequence among nonstructural proteins encoded by RNA viruses that have dissimilar genomic organization. Proc. Natl. Acad. Sci. USA **81**:4358–4362.

18a. **Jones, M. E.** Unpublished data.

19. **Kamer, G., and P. Argos.** 1984. Primary structural comparison of RNA-dependent polymerases from plant, animal, and bacterial viruses. Nucleic Acids Res. **12**:7269–7282.
20. **Kinney, R. M., B. J. B. Johnson, J. B. Welch, K. R. Tsuchiya, and D. W. Trent.** 1989. The full-length nucleotide sequences of the virulent Trinidad donkey strain of Venezuelan equine encephalitis virus and its attenuated vaccine derivative, strain TC-83. Virology **170**:19–30.
21. **Kunkel, T. A.** 1985. Rapid and efficient site-specific mutagenesis without phenotypic selection. Proc. Natl. Acad. Sci. USA **82**:488–492.
22. **Laemmli, U. K.** 1970. Cleavage of structural proteins during the assembly of the head of bacteriophage T4. Nature (London) **227**:680–685.
23. **Laskey, R. A., and A. D. Mills.** 1975. Quantitative film detection of ^{3}H and ^{14}C in polyacrylamide gels by fluorography. Eur. J. Biochem. **56**:335–341.
24. **LaStarza, M. W., A. Grakoui, and C. M. Rice.** 1994. Deletion and duplication mutations in the C-terminal nonconserved region of Sindbis virus: effects on phosphorylation and on virus replication in vertebrate and invertebrate cells. Virology **202**:224–232.
25. **Lemm, J. A., R. K. Durbin, V. Stollar, and C. M. Rice.** 1990. Mutations which alter the level or structure of nsP4 can affect the efficiency of Sindbis virus replication in a host-dependent manner. J. Virol. **64**:3001–3011.
26. **Lemm, J. A., M. E. Jones, G. Li, and M. W. LaStarza.** Unpublished data.
27. **Lemm, J. A., and C. M. Rice.** 1993. Assembly of functional Sindbis virus RNA replication complexes: requirement for coexpression of P123 and P34. J. Virol. **67**:1905–1915.
28. **Lemm, J. A., and C. M. Rice.** 1993. Roles of nonstructural polyproteins and cleavage products in regulating Sindbis virus RNA replication and transcription. J. Virol. **67**:1916–1926.
29. **Lemm, J. A., T. Rümenapf, E. G. Strauss, J. H. Strauss, and C. M. Rice.** Polypeptide requirements for assembly of functional Sindbis virus replication complexes: a model for the temporal regulation of minus and plus-strand RNA synthesis. EMBO J., in press.
30. **Levis, R., S. Schlesinger, and H. V. Huang.** 1990. Promoter for Sindbis virus RNA-dependent subgenomic RNA transcription. J. Virol. **64**:1726–1733.
31. **Li, G., M. W. LaStarza, W. R. Hardy, J. H. Strauss, and C. M. Rice.** 1990. Phosphorylation of Sindbis virus nsP3 *in vivo* and *in vitro*. Virology **179**:416–427.
32. **Li, G., B. Pragai, and C. M. Rice.** 1991. Rescue of Sindbis virus-specific RNA replication and transcription by using a vaccinia virus recombinant. J. Virol. **65**:6714–6723.
33. **Li, G., and C. M. Rice.** 1989. Mutagenesis of the in-frame opal termination codon preceding nsP4 of Sindbis virus: studies of translational readthrough and its effect on virus replication. J. Virol. **63**:1326–1337.
34. **Maniatis, T., E. F. Fritsch, and J. Sambrook.** 1982. Molecular cloning: a laboratory manual. Cold Spring Harbor Laboratory, Cold Spring Harbor, N.Y.
35. **Mi, S., R. Durbin, H. V. Huang, C. M. Rice, and V. Stollar.** 1989. Association of the Sindbis virus RNA methyltransferase activity with the nonstructural protein nsP1. Virology **170**:385–391.
36. **Mi, S., and V. Stollar.** 1991. Expression of Sindbis virus nsP1 and methyltransferase activity in *Escherichia coli*. Virology **184**:423–427.
37. **Novak, J. E., and K. Kirkegaard.** 1991. Improved method for detecting poliovirus negative strands used to demonstrate specificity of positive-strand encapsidation and the ratio of positive to negative strands in infected cells. J. Virol. **65**:3384–3387.
38. **Pierce, J. S., E. G. Strauss, and J. H. Strauss.** 1974. Effect of ionic strength on the binding of Sindbis virus to chick cells. J. Virol. **13**:1030–1036.
39. **Raju, R., and H. V. Huang.** 1991. Analysis of Sindbis virus promoter recognition in vivo, using novel vectors with two subgenomic mRNA promoters. J. Virol. **65**:2501–2510.
40. **Rice, C. M., R. Levis, J. H. Strauss, and H. V. Huang.** 1987. Production of infectious RNA transcripts from Sindbis virus cDNA clones: mapping of lethal mutations, rescue of a temperature-sensitive marker, and in vitro mutagenesis to generate defined mutants. J. Virol. **61**:3809–3819.
41. **Saiki, R. K., D. H. Gelfand, S. Stoffel, S. J. Scharf, R. Higuchi, G. T. Horn, K. B. Mullis, and H. A. Erlich.** 1988. Primer-directed enzymatic amplification of DNA with a thermostable DNA polymerase. Science **239**:487–491.
42. **Sanger, F., S. Nicklen, and A. R. Coulson.** 1977. DNA sequencing with chain-terminating inhibitors. Proc. Natl. Acad. Sci. USA **74**:5463–5467.
43. **Sawicki, D. L., D. B. Barkhimer, S. G. Sawicki, C. M. Rice, and S. Schlesinger.** 1990. Temperature sensitive shut-off of alphavirus minus strand RNA synthesis maps to a nonstructural protein, nsP4. Virology **174**:43–52.
44. **Sawicki, D. L., and S. G. Sawicki.** 1985. Functional analysis of the A complementation group mutants of Sindbis HR virus. Virology **144**:20–34.
45. **Sawicki, D. L., and S. G. Sawicki.** 1993. A second nonstructural protein functions in the regulation of alphavirus negative-strand RNA synthesis. J. Virol. **67**:3605–3610.
46. **Sawicki, D. L., S. G. Sawicki, S. Keränen, and L. Kääriäinen.** 1981. Specific Sindbis virus-coded functions for minus-strand RNA synthesis. J. Virol. **39**:348–358.
47. **Sawicki, S. G., D. L. Sawicki, L. Kääriäinen, and S. Keränen.** 1981. A Sindbis virus mutant temperature-sensitive in the regulation of minus-strand RNA synthesis. Virology **115**:161–172.
48. **Scheidel, L. M., and V. Stollar.** 1991. Mutations that confer resistance to mycophenolic acid and ribavirin on Sindbis virus map to the nonstructural protein nsP1. Virology **181**:490–499.
49. **Schlesinger, S., and M. J. Schlesinger (ed.).** 1986. The Togaviridae and Flaviviridae. Plenum Press, New York.
50. **Shirako, Y., and J. H. Strauss.** 1990. Cleavage between nsP1 and nsP2 initiates the processing pathway of Sindbis virus nonstructural polyprotein P123. Virology **177**:54–64.
51. **Shirako, Y., and J. H. Strauss.** 1994. Regulation of Sindbis virus RNA replication: uncleaved P123 and nsP4 function in minus-strand RNA synthesis, whereas cleaved products from P123 are required for efficient plus-strand RNA synthesis. J. Virol. **68**:1874–1885.
52. **Simmons, D. T., and J. H. Strauss.** 1972. Replication of Sindbis

virus. II. Multiple forms of double-stranded RNA isolated from infected cells. J. Mol. Biol. **71**:615–631.
53. **Strauss, E. G., R. J. deGroot, R. Levinson, and J. H. Strauss.** 1992. Identification of the active site residues in the nsP2 proteinase of Sindbis virus. Virology **191**:932–940.
54. **Strauss, E. G., E. M. Lenches, and J. H. Strauss.** 1976. Mutants of Sindbis virus. I. Isolation and partial characterization of 89 new temperature-sensitive mutants. Virology **74**:154–168.
55. **Strauss, E. G., R. Levinson, C. M. Rice, J. Dalrymple, and J. H. Strauss.** 1988. Nonstructural proteins nsP3 and nsP4 of Ross River and O'Nyong-nyong viruses: sequence and comparison with those of other alphaviruses. Virology **164**:264–274.
56. **Strauss, E. G., C. M. Rice, and J. H. Strauss.** 1983. Sequence coding for the alphavirus nonstructural proteins is interrupted by an opal termination codon. Proc. Natl. Acad. Sci. USA **80**:5271–5275.
57. **Strauss, E. G., C. M. Rice, and J. H. Strauss.** 1984. Complete nucleotide sequence of the genomic RNA of Sindbis virus. Virology **133**:92–110.
58. **Strauss, E. G., and J. H. Strauss.** 1980. Mutants of alphaviruses: genetics and physiology, p. 393–426. *In* R. W. Schlesinger (ed.), The togaviruses. Academic Press, New York.
59. **Strauss, J. H., and E. G. Strauss.** 1990. Alphavirus proteinases. Semin. Virol. **1**:347–356.
60. **Takkinen, K.** 1986. Complete nucleotide sequence of the nonstructural protein genes of Semliki Forest virus. Nucleic Acids Res. **14**:5667–5682.
61. **Wang, Y., S. G. Sawicki, and D. L. Sawicki.** 1991. Sindbis virus nsP1 functions in negative-strand RNA synthesis. J. Virol. **65**:985–988.
62. **Wang, Y. F., S. G. Sawicki, and D. L. Sawicki.** Alphavirus nsP3 functions to form replication complexes transcribing negative-strand RNA. J. Virol., in press.

JOURNAL OF VIROLOGY

SEPTEMBER 1994
VOL. 68, NO. 9

PUBLISHED MONTHLY BY
THE AMERICAN
SOCIETY FOR MICROBIOLOGY